Khulna University Studies Volume 21(1): 162-177: 2024

ORIGINAL ARTICLE

LIFE SCIENCE

NATURAL ALKANES FROM *Senna siamea* AS POSSIBLE CONTENDERS AGAINST INFLAMMATORY DISORDERS: AN *IN SILICO* AND METABOLOMICS PERSPECTIVE

Arindam Ghosh[1], Sourav Chakraborty[1&2], Soumya Majumder[1], Sahadeb Sarkar[1] and Malay Bhattacharya[1*]

[1]*Molecular Biology and Tissue Culture Laboratory, Department of Tea Science, University of North Bengal, Siliguri, West Bengal, 734013, India*

[2]*Department of Botany, Darjeeling Government College, Darjeeling, West Bengal, 734101, India*

KUS: 1109: 02122023

Manuscript submitted: December 2, 2023 Accepted: June 10, 2024

Abstract

Inflammation is a response to host tissue injury occurring due to irritants or pathogenic infections. It increases levels of cytokines, immune-regulatory factors, cytokine receptors, etc. Cyclooxygenase (COX-1, COX-2, and COX-3) is an enzyme responsible for the formation of prostaglandins. So, by inhibiting this cyclooxygenase-2 enzyme, the treatment of inflammation disorders may be more accessible. *Senna siamea* is a well-known medicinally important tea plantation shade tree that has anti-inflammatory properties. GC-MS was done to find out the secondary metabolites present in the acetone extract of leaves. Alkanes like undecane,3,8-dimethyl; 2-methyltetracosane, hexadecane, heneicosane, etc. were predominantly detected by GC-MS. *In silico* studies of eicosane and heptadecane were conducted against pro-inflammatory cytokines like tumor necrosis factor, interleukin-6, and mediator cyclooxygenase. Molecular docking results showed that the two compounds are potential inhibitors of inflammation where eicosane had better binding affinity against all the selected proteins than heptadecane, with both having only one Lipinski violation. Molsoft, Molinspiration, and Swiss-ADMET software were applied to evaluate the two compounds' possible physicochemical, drug-like, and ADMET features. These two compounds can be developed and used as effective inhibitory agents against inflammation; however, more *in vitro* and *in vivo* research is needed before conducting clinical trials. Besides the metabolomics-based biosynthesis pathway of two compounds, biosynthetic pathways of other detected compounds were also established, which might help the scientific community to increase the yield of these compounds via the methodology of metabolic bioengineering in order to develop novel pharmaceutical products.

Keywords: GC-MS, Metabolites, Biosynthesis, *In-silico*, ADMET

Introduction

Inflammation is a response or defense system of any host tissue that rises when the tissues get injured or infected. This is usually caused by the increased level of cytokines, immune-regulatory factors, cytokine receptors, etc. During inflammation, changes like swelling, redness, itching, pain, etc. in the tissue happen. The enzyme cyclooxygenase, often known as COX, is in charge of converting arachidonic acid into prostaglandins, also known as prostanoids. The enzymes COX-1, COX-2, and COX-3 are the three isoforms of this cyclooxygenase (Gunalan et al., 2014). Between these three isoenzymes, COX-2 is inducible and is the main reason behind inflammation disorder. So, by inhibiting this COX-2 enzyme, the treatment of inflammation disorder would be more accessible. Most inflammatory conditions, including gout and arthritis, are treated with non-steroidal anti-inflammatory medications (NSAIDs) to get relief from pain, but continuous use of these NSAIDs has serious side effects like gastroduodenal erosions, ulceration, myocardial infarction, nephrotoxicity, etc. (Joshi et al., 2020, Hassan et al., 2022). Therefore, the treatment of inflammatory disorders without any or fewer side effects still needs to be resolved and has become a growing concern to the scientific community. Thus, new anti-inflammatory drugs which can inhibit COX-2, need to be developed. Plants have always played a central role in the treatment of various diseases throughout the world. The traditional use of medicine is

*Corresponding author: <malaytsnbu@gmail.com>

DOI: https://doi.org/10.53808/KUS.2024.21.01.1109-ls

prevalent where plants play a huge role by providing bioactive molecules that might lead us to develop novel drugs to treat various diseases.

Senna siamea (Lam.) Irwin et Barneby also known as *Cassia siamea* (Fabaceae), is a tropical fast-growing evergreen native plant from southeast Asian countries like India, Cambodia, Thailand, Brunei, Myanmar, Malaysia, Nepal, Philippines, Sri Lanka, etc. The generic name of this plant means spice and the species is stated to have originated in Thailand. This plant is also used as a shade tree in the tea plantations of various parts of India. It is also used as an ornamental plant and the wood is used as timber, fuels, furniture, etc. (Kumar et al., 2017). This plant has many phytochemical components and acts as a medicinal plant as it is reported to cure hepatic complications, loss of appetite, insomnia etc. (Veerachari and Bopaiah 2011). Barakol, a significant compound from this plant, has been reported as having sedative and anxiolytic activity (Sukma et al., 2002). Curry made from its leaves is a very popular cuisine in Thailand (https://en.wikipedia.org/wiki/Senna_siamea). Burmese households traditionally gather its buds on the full moon day of Tazaungmon (8th month of traditional Burmese calendar) and use them to make a salad called mezali phu thoke (https://en.wikipedia.org/wiki/Senna_siamea). In Malaysia, the stem or stem bark of *S. siamea*, also known as "Sebusok" or "Johor", is utilised as a beverage or for bathing to combat malaria and liver ailments. In Uganda, the leaves of the plant, usually referred to as "Mjohoro," are frequently used for the treatment of gastrointestinal discomfort (Kamagaté et al., 2014). Leaves of this plant are reported to have antiviral as well as antinociceptive activity and cure ringworm-related skin disorders. The stem bark has an anti-inflammatory effect (Mehta et al., 2017). Compounds like cassiarin A, cassiarin B, D-pinitol, luteolin, lupeol, 2',4',5,7-tetrahydroxy-8-C-glucosylisoflavone and piceatannol, chrysophanol, emodin, betulinic acid etc. have been found in the leaves and stem bark respectively (Kamagaté et al., 2014). *In silico* or computational biological study delivers the possibility of exploring the interaction between protein and bioactive molecules as a ligand. This rapid computational docking study is very useful for the discovery of novel drugs. This study was planned to distinguish the bioactive molecules present in Senna leaves and their biosynthesis process prior to targeting inflammatory proteins by using molecular docking tactics with ADME-Tox analysis.

Materials and Method

Collection and preparation of sample

Young, healthy, fresh leaves were separated from mature shoots, collected in ziplock bags, kept in a box packed with ice, and taken to the laboratory for further studies. The leaves were then washed with distilled water to get rid of dust particles and the surface was dried out with tissue paper prior to crushing in liquid nitrogen and dissolved in acetone to make the extract. The extract was stored at 25 °C on a shaker for a whole day. The supernatant was then collected after centrifugation, followed by gas chromatography-mass spectrometry analysis.

Analysis of Gas chromatography-mass spectrometry

Acetone extract with a concentration of 25 mg/ml was used for GC-MS. GC-MS analysis was done by following the protocol of Majumder et al. (2020) and Ghosh et al. (2021). One microliter of the sample was injected in a split mode in GCMS-QP2010 Plus. Injection temperature, interface temperature, and ion source temperature were set at 260 °C, 270 °C, and 230 °C, respectively. Helium gas was used as a carrier. TFR (total flow rate) was 16.3 ml/min, while CFR (column flow rate) was 1.21 ml/min. The recording rate of mass spectra was 5 scan/s with a scanning range of 40-650 m/z. Compound identification was done using library databases like NIST08s.LIB and WILEY8.LIB. The peak area was considered for the quantification of each compound. The peak report obtained from GC-MS analysis was further studied from the available literature.

Bioactive compounds obtained from the extract and study on their biosynthesis pathway

Studies on biosynthesis pathways of different bioactive compounds detected in GC-MS were done by reviewing various available literature (Majumder et al., 2022) and databases like GenBank, KEGG 2023, Genomes database 2023 and PubChem 2023.

Molecular properties and drug-likeness features of probable drug candidates

Molinspiration (http://www.molinspiration.com/) a computational tool, was used to find out the molecular properties and drug likeness characteristics of the two reported anti-inflammatory biomolecules detected in *Senna siamea* in the form of partition coefficient (miLogP), topological polar surface area (TPSA), number of atoms (n-

atoms), Molecular weight, number of hydrogen bond receptor, number of hydrogen bond donor (nOHNH), number of rotatable bonds (nrotb), molecular volume, in addition to these, the bioactivity scores were determined concerning their efficacy as ion channel modulator, nuclear receptor ligand, kinase inhibitor, G-protein coupled receptor (GPCR) ligand, protease, and enzyme inhibitor. Two query compounds were further executed for *in silico* investigation by using another online server Molsoft (http://www.molsoft.com/), which provides a drug-likeness model score of the respective test molecules as well as gives a graphical representation of biomolecular properties.

Protein and ligand structure selection and modeling

Eicosane and heptadecane (reported as anti-inflammatory) detected by GC-MS in *Senna siamea* were chosen as probable anti-inflammatory candidates for molecular docking analysis against human inflammatory disease proteins like COX-1, COX-2, IL-6, and TNF. Ibuprofen was also selected as a standard anti-inflammatory drug. The X-ray diffraction crystal structures of (6Y3C; 3.361 Å), (5F19; 2.04 Å), (1ALU; 1.90 Å), and (5MU8; 3.00 Å) were selected and retrieved from the PDB (protein data bank). Water molecules were erased and Kollman charges were added in Auto dock tools to do a flawless interaction. The three-dimensional structures of the preferred alkanes were retrieved from the PubChem database (https://pubchem.ncbi.nlm.nih.gov/). Ultimately, AutoDock Vina was used for the molecular docking process, while Ligplot+ was used for interaction studies.

ADME-Tox prediction

The ADMET evaluation gives an indistinct idea about the probable side effects and the related health impact as this feature of ADMET predicts hepatic toxicity, metabolic role, membrane transport features, and minimum recommended therapeutic dose of the tested molecules which is correlated with biological effectiveness and their metabolic effect. This was done by using Variable Nearest Neighbor ADMET (vNN-ADMET) (https://vnnadmet.bhsai.org/vnnadmet/home.xhtml), SwissADME (http://www.swissadme.ch/) tool following Ghosh et al., 2022.

BOILED-Egg model properties

A quick and simple way to predict human gastrointestinal absorption and molecule access to the brain for drug development is provided by the Brain or Intestinal Estimated Permeation Predictive Model (BOILED-Egg), also called the Egan egg model. It is based on lipophilicity (water partition coefficient, WLOGP) and polarity (topological polar surface area, TPSA). The SwissADME online web server was also used to create this model of the two query molecules.

Bioavailability radar

Both the probable candidates were assessed in a comprehensive way by taking six physiochemical properties (Dissolvability, Measure, Extremity, Lipophilicity, Adaptability and Immersion) into thought and shaping a bioavailability radar utilizing the SwissADME. The area shaded in pink delineates the ideal ranges for the six parameters. Significant deviations from these ranges on a considerable scale imply that the ligand might not be suitable for oral bioavailability (Garg et al., 2020).

Results and discussion

GC-MS detected compounds

The chromatogram revealed a total of twenty-four peaks (**Table 1**), representing twenty-two distinct chemicals, of which eighteen have been reported as bioactive. Two diterpene (phytol; neophytadiene) and two sterols (Stigmasta-5,23-dien-3-ol, (3beta.)- and. gamma.-Sitosterol) compounds exhibited the major peak area. However, a large area was occupied by the long-chain hydrocarbon, as most of the compounds are alkane in nature (**Figure 2**).

Compounds were classified based on their nature with respect to the biosynthetic pathway, mainly long-chain hydrocarbons, terpenoids, sterols, and others. Interestingly, more than 57.14% of the extracts belong to a number of twelve long-chain hydrocarbons which comprise alkane, alkene, fatty acids, fatty alcohol, and fatty aldehyde, whereas terpenoids and sterols comprise 19% and 10%, respectively (**Figure 2**). But, depending on the peak area, terpenoids share over 47% followed by long-chain hydrocarbons, sterols and others with 27.34%, 18.68% and 6.25%, respectively (**Figure 3**).

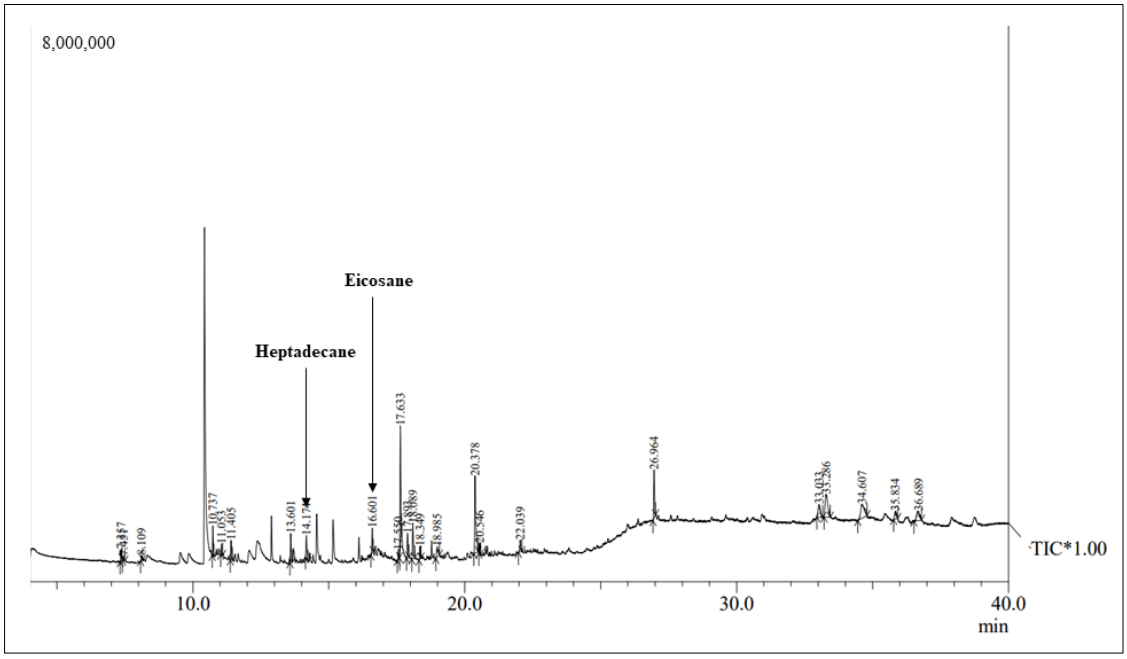

Figure 1. GC-MS chromatogram of the acetone leaf extracts

Table 1. GC-MS detected leaf extract compounds

Peak area%	Retention time	CS leaf GC-MS	MW (g/mol)	Nature	Group
1.31	7.357	Undecane, 3,8-dimethyl-	184.36	Alkane	Long chain hydrocarbons
0.54	7.451	Decane, 3,7-dimethyl-	170.33	Alkane	
0.58	8.109	3-Ethyl-3-methylheptane	142.28	Alkane	
2.86	10.737	Dodecane, 4,6-dimethyl-	198.39	Alkane	
1.15	11.053	2-Methyltetracosane	352.7	Alkane	
2.44	11.405	Hexadecane	226.44	Alkane	
3.45	13.601	Heneicosane	296.6	Alkane	
3.13	14.174	Heptadecane	240.5	Alkane	
4.38	16.601	Eicosane	282.5	Alkane	
1.07	17.550	(2e)-3,7,11,15-tetramethyl-2-hexadecene	280.5	Alkene	
1.85	22.039	Glycidyl palmitate	312.5	Fatty acid ester	
4.58	33.033	Eicosanal-	296.5	Fatty aldehyde	
15.77	17.633	Neophytadiene	278.5	Diterpene	Terpenoids
20.72	20.378	Phytol	296.5	Diterpene	
6.59	26.964	Squalene	410.7	Triterpene	
4.62	36.689	24-Norursa-3,12-diene	394.7	Pentacyclic triterpene	
10.20	33.286	Stigmasta-5,23-dien-3-ol, (3.beta.)-	412.7	Phytosterol	Sterols
8.48	34.607	.gamma.-Sitosterol	414.7	Phytosterol	
1.00	20.546	l-Norvaline, N-(2-methoxyethoxycarbonyl)-, tetradecyl ester	415.6	Alpha-amino acid	Others
2.91	18.985	1,2-benzenedicarboxylic acid, dibutyl ester	278.34	Carboxylic acid	
2.34	35.834	Unidentified		-----	

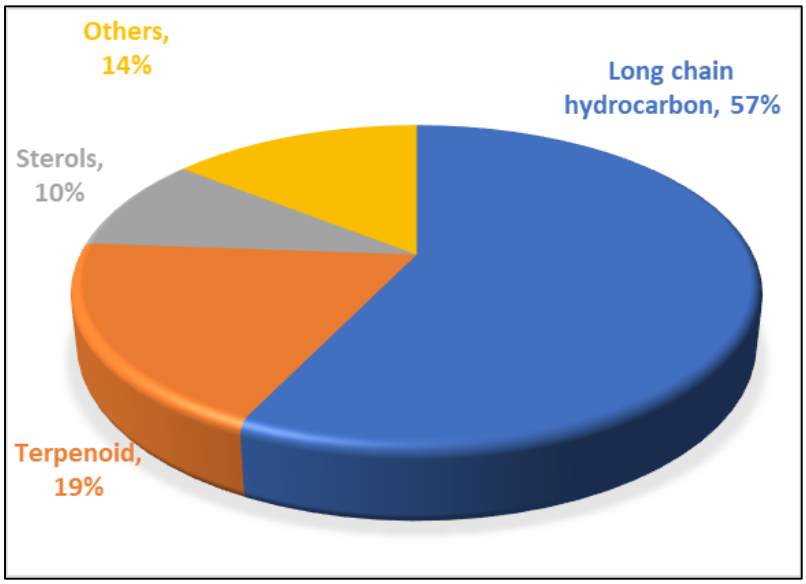

Figure 2. Contribution of chemical groups of compounds on the basis of their presence

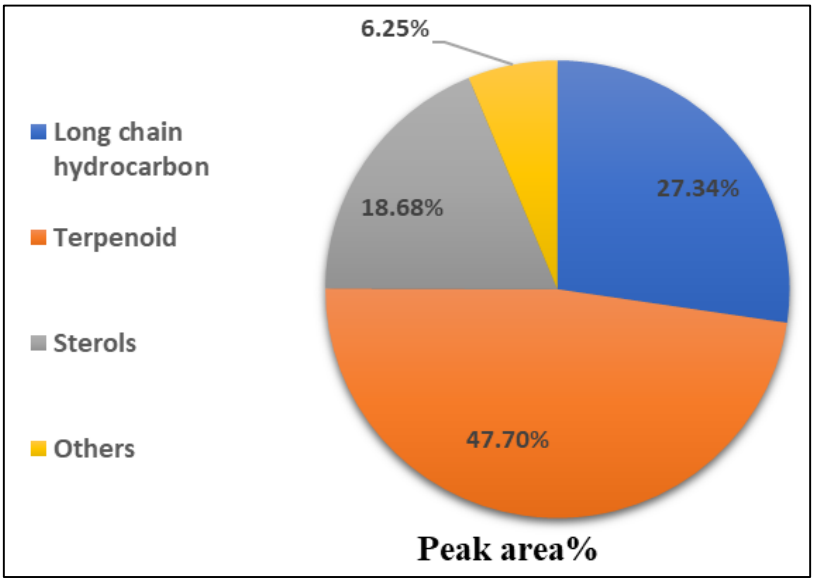

Figure 3. Contribution of chemical groups of compounds based on the percentage of their peak area

Biosynthesis of GC-MS detected terpenoid compounds

Two diterpenoids viz. phytol and neophytadiene have been detected in the leaf sample with a peak area percentage of 20.72% and 15.77%. Phytol, a diterpenoid alcohol that is produced from geranylgeranyl diphosphate (GGPP) with the presence of geranylgeranyl diphosphate synthase (EC 2.5.1.29) and neophytadiene which is another diterpenoid detected in our sample may be formed after the removal of water from phytol in the cell chloroplast.

Dimethylallyl pyrophosphate (DMAPP) is formed from isopentenyl diphosphate (IPP), with the help of isopentenyl-diphosphate delta-isomerase (EC 5.3.3.2). After that, IPP molecule and DMAPP molecule combine to make farnesyl diphosphate (FPP). From that FPP, detected terpenoid squalene is formed with the help of farnesyl-diphosphate farnesyltransferase (EC 2.5.1.21) having pre-squalene diphosphate as an intermediate which then enters into triterpenoid biosynthesis. Squalene mono-oxygenase (E.C. 1.14.14.17) is an enzyme that helps to synthesize 2,3-

oxidosqualene which enters into triterpenoid and steroid biosynthesis pathway as well, in the mitochondria (Chakraborty et al., 2022).

24-Norursa-3,12-diene (peak area of 4.62%), a dammarenyl-type pentacyclic triterpene detected through gcms is a derivative of β-boswellic acid (Hanuš et al., 2007), which is synthesized from alpha-amyrin (Ahmed et al., 2021) with having 2,3-oxidosqualene as a precursor in the triterpenoid biosynthesis pathway.

In the steroid biosynthesis pathway, 2,3-oxidosqualene gets converted to cycloartenol and by a long series of reactions produce sitosterol (detected as. gamma. -sitosterol) and with the engagement of sterol 22-desaturase, stigmasterol (Stigmasta-5,23-dien-3-ol, (3.beta.)-) is biosynthesized with the peak area of 8.48% and 10.20% respectively (**Figure 4**, **Table 1**).

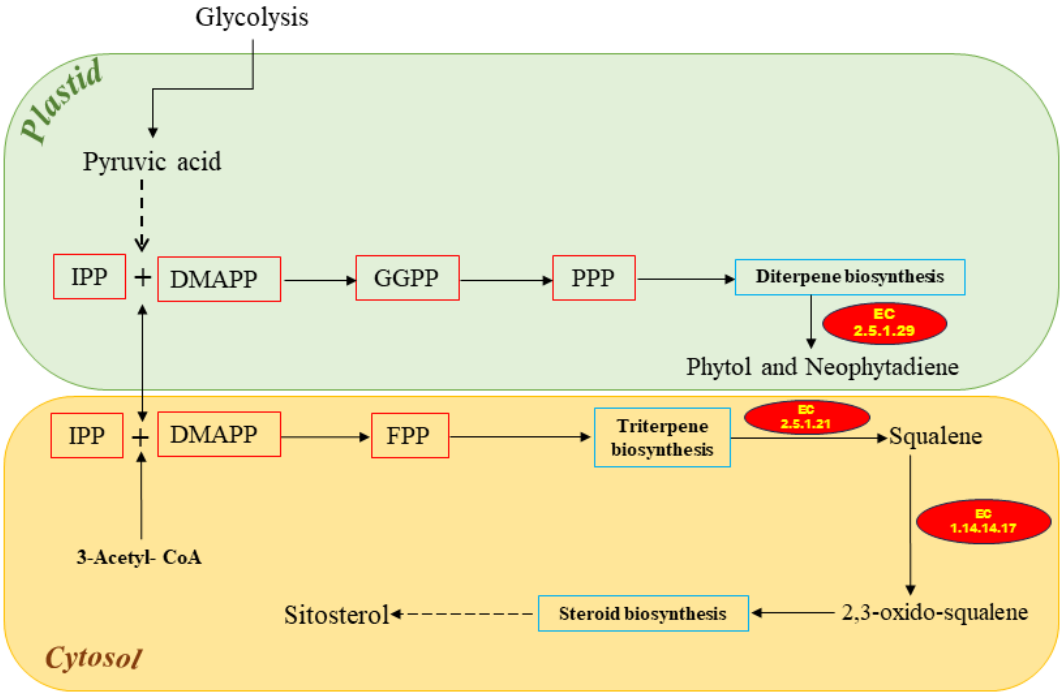

Figure 4. Biosynthesis pathway of terpenoids detected through GC-MS

Biosynthesis of GC-MS detected long-chain hydrocarbon compounds

In our study, a total of twelve long-chain hydrocarbons like alkanes, alkenes, fatty aldehydes were detected. The alkanes were found to be the highest detected compounds group with a share percentage of seventy-five. The rest of the contribution are equally shared by the alkene, fatty aldehyde, and fatty acid ester. Out of twelve long-chain hydrocarbons, four compounds followed the cutin, suberin, and wax biosynthesis pathway via the odd-chain fatty acid elongation pathway. Three-carbon compound propionyl Co-A is the precursor of odd-chain fatty acids metabolism, where the pathway is different from the even-chain fatty acids synthesis. Propionyl Co-A is formed as a result of the breakdown of odd-chain fatty acids in peroxisomes, the degradation of chlorophyll in plastids, and the catabolism of amino acids such as valine and isoleucine (Hildebrandt et al., 2015; Lucas et al., 2007). Derivatives of odd chain fatty acids like heptane (C7) as 3-ethyl-3-methylheptane, undecane (C11) as undecane, 3,8-dimethyl-, heptadecane (C17), heneicosane (C21) were detected in the leaf extracts through GC-MS.

In general, the biosynthesis of odd-chain fatty acids arises in the chloroplast by the condensation of propionyl Co-A and malonyl Co-A with the help of beta-ketoacyl-ACP synthase III to form 5-carbon compound 3-oxovaleryl-ACP with carbon dioxide as a secondary product (Brown et al., 2009). This 3-oxovaleryl-ACP acts as the precursor molecule for the initiation of odd chain fatty acids elongation process and by attachment of malonyl ACP (M-ACP) as two carbon units in each following round produces successive odd chain fatty acids like heptanoic acid and

undecanoic acid whereas, heptadecanoic acid and heneicosanoic acid are also synthesized in a similar way but in the smooth endoplasmic reticulum (Chakraborty et al., 2022). Heptadecanoic acid is converted to heptadecanal (long-chain aldehyde) with the help of a reduction enzyme aldehyde dehydrogenase, and ultimately produces heptane detected as 3-Ethyl-3-methylheptane aided by aldehyde decarbonyalse enzyme (EC 4.1.99.5); similarly, undecane detected as undecane, 3,8-dimethyl-, is produced from its corresponding aldehyde undecanal which is derived from undecanoic or undecyclic acid. Another report has shown that in *E. coli*, the Lauroyl-ACP is converted to lauric acid with the help of lauroyl-ACP thioesterase (Lauroyl-ACP thioesterase - Definition of lauroyl-ACP thioesterase (healthbenefitstimes.com)) then by following general cutin, suberin and wax biosynthetic pathway, it is converted to dodecanal and by the decarbonylation process it finally yields undecane, where fatty acyl-CoA synthetase, fatty acyl-reductase and fatty aldehyde decarbonylase are involved (Yan et al., 2016). Being a precursor, 3-oxovaleryl-ACP elongates by adding a series of malonyl-ACP into pentadecanoic acid and after that by adding two carbon malonyl CoA in each subsequent cycle heptadecanoic acid is formed in the endoplasmic reticulum and finally follows cutin, suberin and wax biosynthesis pathway to yield heptadecane (detected through GC-MS) and another study on the leguminous plant *Pisum sativum* showed that heptadecane could be synthesized directly from octadecanal with the release of CO by the involvement of aldehyde decarbonylase (Schneider-Belhaddad & Kolattukudy 2000, Iqbal et al., 2022). Heneicosane, another detected long-chain alkane, is probably synthesized from its previous counterparts nonadecanoic acid, in a similar way as described in the case of heptadecane; although no reports were found regarding the biosynthesis of this particular compound.

Out of twelve long-chain hydrocarbons, eight compounds viz. decane, 3,7-dimethyl-; dodecane, 4,6-dimethyl-; hexadecane; (2e)-3,7,11,15-tetramethyl-2-hexadecene; glycidyl palmitate; eicosane and eicosanal- are the derivatives of even chain fatty acids. Biosynthesis of even chain fatty acids is initiated in the mitochondria with the help of acetyl-CoA carboxylase, Acetyl CoA is transformed to malonyl-CoA followed by biosynthesis of M-ACP with the involvement of malonyl transcylase. The condensation of this M-ACP with acetyl-ACP with the help of acetyl transacylase (EC 2.3.1.38) yields acetoacetyl-ACP. After the reduction of acetoactyl-ACP with the engagement of β-ketoacyl-ACP reductase (EC 1.1.1.100) and enoyl-ACP (EC 1.3.1.10) through a long reaction, it finally produces a 4-carbon compound butyryl-ACP. This is the first step of the elongation process by the addition of two carbon units M-ACP, extending the acyl-ACP chain in each following cycle. This cycle is continuously happening until the synthesizing of palmitoyl-ACP or hexadecanoyl-ACP (C-16) with decanoyl-ACP (C10) and dodecanoyl-ACP (C-12) as major intermediate compounds. Any acyl-CoA is converted to aldehyde and then alkane with the help of long-chain-aldehyde dehydrogenase (EC 1.2.1.48) and long-chain acyl-protein thioester reductase (EC 1.2.1.50) by the involvement of luxC gene. After the formation of palmitoyl-ACP, the acyl-malonyl-ACP condensing enzyme cannot extend this elongation process in a similar way as previously shown, instead, the enzyme thioesterase (EC 3.1.2.14) plays a part here and produces palmitate and ACP. In our study, we detected palmitic acid as glycidyl palmitate, which is formed from palmitoyl-ACP with the help of palmitoyl-CoA hydrolase (EC 3.1.2.2). After the desaturation of palmitic acid to palmitoleic acid with the help of stearoyl-CoA desaturase-1 and then in the presence of long chain acyl–protein thioester reductase/long-chain aldehyde dehydrogenase, it is further reduced to hexadecenal and lastly synthesize hexadecene (detected as (2e)-3,7,11,15-tetramethyl-2-hexadecene) by aldehyde decarbonylase. Two carbon donor malonyl CoA with enzymes located in smooth endoplasmic reticulum plays a role beyond C-16 palmitate production, which ends up in the elongation of octadecanoyl CoA (C-18), eicosanoyl CoA (C-20), docosanoyl CoA(C-22), tetracosanoyl CoA (C-24) and so on. Another detected alkane, decane, 3,7-dimethyl- is produced from decanoyl CoA with the help of aldehyde decarbonylase having the intermediate of decanal. Similarly, other alkanes like dodecane, hexadecane, eicosane, and tetracosane detected in our study are synthesized by following the similar cutin, suberin, and wax biosynthesis pathway where aldehyde decarbonylase played a major role. A summary view of the proposed origin of long-chain hydrocarbons and their derivatives is provided in **Figure 5**.

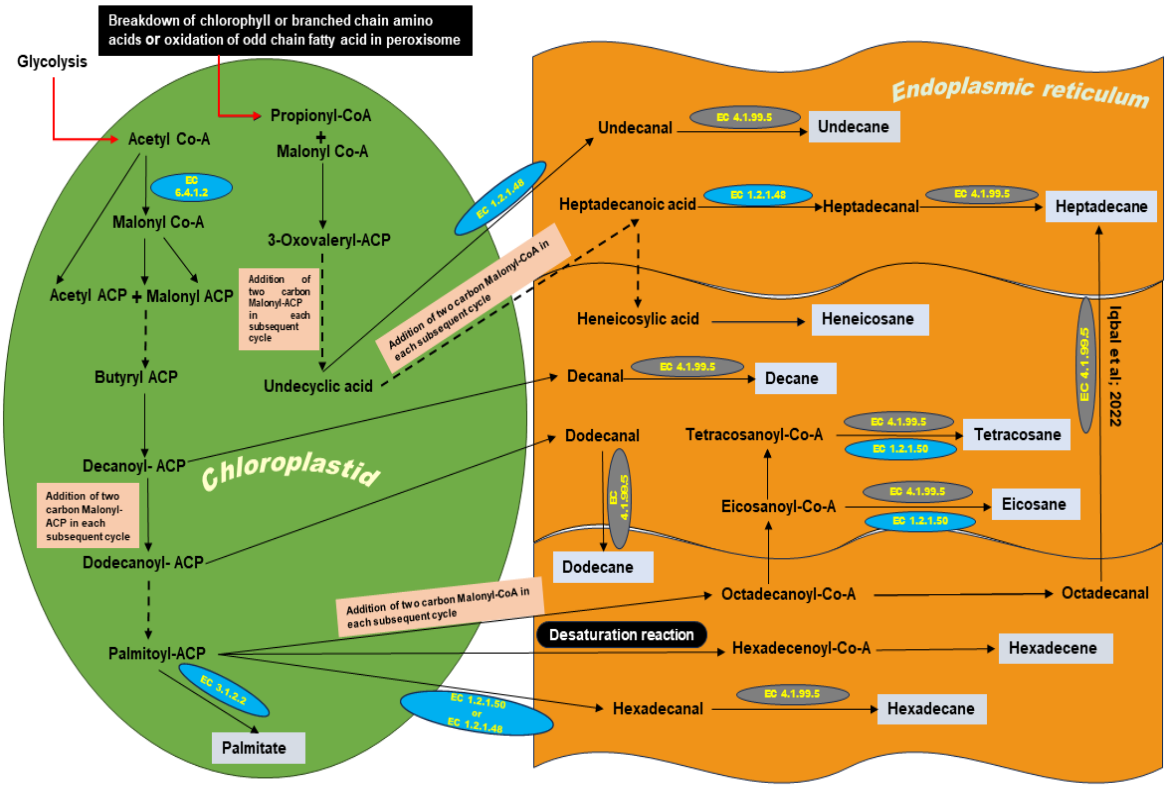

Figure 5. Probable biosynthesis pathway of detected long chain hydrocarbons through GC-MS (Dotted arrow depicts long steps, enzyme catalogue numbers involved are provided in round coloured boxes)

Characterization of ADMET properties of query molecules

By using the Swiss ADME and vNN ADMET, the pharmacokinetic characteristics of the two chosen drugs were evaluated in the form of ADME-Tox predictions. ADMET influences the maximum recommended therapeutic dose and exposure of drugs to the apprehensive tissue system. Our ADMET prediction represents that eicosane has three instances of negative output, whereas heptadecane has been found to have two instances of negative output (**Table 2**).

Table 2. ADME-Toxicity study of the probable drug compounds (Eicosane and Heptadecane)

ADMET study parameter		Eicosane	Heptadecane
Liver toxicity	DILI	No	No
	Cytotoxicity	No	No
Metabolism (Cyp inhibitors for)	HLM	No	No
	1A2	No	No
	3A4	No	No
	2D6	No	No
	2C9	No	No
	2C19	No	No
Membrane transporters	BBB	Yes	Yes
	P-gp inhibitor I	No	No
	P-gp inhibitor II	Yes	No
	P-gp substrate	Yes	Yes
Others	hERG blocker	No	No
	MMP*	No	No
	AMES	No	No

	MRTD (mg/day)	211	180

Molecular properties of selected drug compounds computed through Molsoft

Graphical representation (**Figure 6**) depicts the drug-likeness model scores, which were evaluated using Molsoft software program, where green colored line represents non drug like behavior by showing positive values and the blue color specifies drug-like traits by displaying zero or negative values (Shaik et al., 2019). Both the concerned molecules were found negative drug likeness model scores with a value of -1.03. The other parameters like BBB (blood-brain barrier) score for the two compounds were very closely related, where eicosane showed a score of 1.34 and heptadecane showed a 1.31 BBB score. BBB score signifies the drug-likeness of the concerned molecule and its ability to penetrate the BBB.

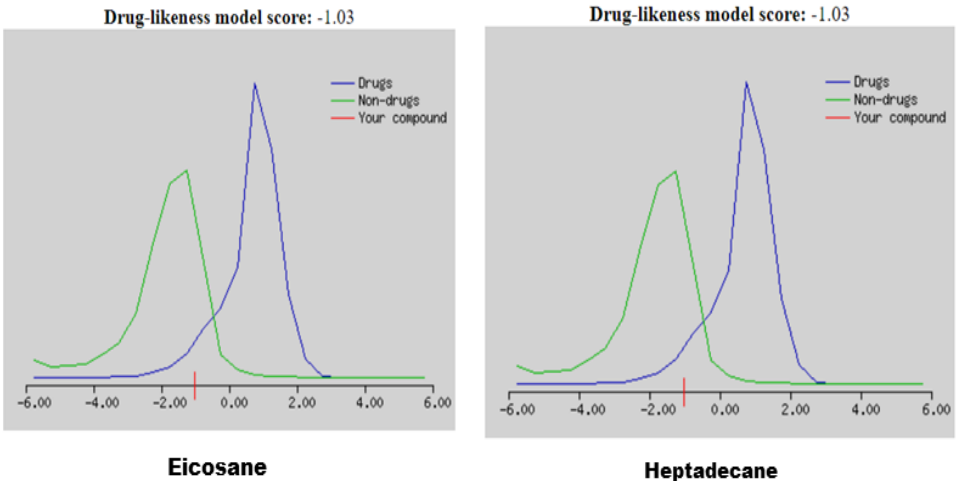

Figure 6. Drug-likeness model score of Eicosane and Heptadecane

Physicochemical properties of probable anti-inflammatory candidates

The physiochemical traits of eicosane and heptadecane were examined by *in silico* method for evaluation of miLogP (Octanol-water partition coefficient) value, weight of the molecule, number of Hydrogen bond acceptors and donors along with the amount of rotatable bonds. The manifold features of the prospective anti-inflammatory molecules were assessed according to Lipinski's rule of five, which depicts numerical values as multiples of 5, corresponding to drug-like characteristics. According to Lipinski's rule of five, to be effective in modulating cell function, potent compounds that are expected to be effective as drug molecules should have superior plasma membrane permeability with a measure of LogP≤5, molecular weight≤500, number of hydrogen bond acceptors≤10, and number of hydrogen bond donors≤5. It is possible to think of molecules that violate more than one of these criteria as less probable therapeutic targets. The two compounds detected in *Senna siamea* were evaluated by several parameters after determining that they were possible drug targets, and none of the compounds showed more than two cases of violation of Lipinski's rule of five (**Table 3**). Biophysical scores of the target molecules are as follows with partition coefficient (miLogP) values of 8.79 to 9.32, molecular weights (MW) of 240.475 to 282.556 KDa, and numbers of hydrogen bond donors and acceptors zero, the number of rotatable bonds (RB) investigated were between 14 and 17, and the molecular weight was investigated below 348.19 g/mol. The number of rotatable bonds determines the flexibility of the drug molecules, which influences the binding mechanism of the ligand molecule to each receptor protein, as previously reported (Priya et al., 2015; Ghosh et al., 2022) that to qualify a drug for the oral bioavailability, the number of rotatable bonds in the drug target must be 10 or less. The molecules we tested have a higher number of rotatable bonds.

Table 3. Physicochemical parameters of query drug targets

	Drug evaluation	Eicosane	Heptadecane
Molecular physicochemical property	MiLogP	9.32	8.79
	TPSA (Å)	0.00 Å	0.00 Å
	n-atoms	20	17
	Volume (g/mol)	348.19	297.78
	Water solubility (log mol/L)	-8.59	-8.337
	Caco2 permeability (log Papp in 10-6 cm/s)	1.371	1.374
	Intestinal absorption	89.671%	90.702%
	Skin permeability (log Kp)	-2.774	-2.517
	Molecular weight	282.556	240.475
	Log p	8.048	6.8777
	Rotatable bonds	17	14
	H-acceptors	0	0
	H-donors	0	0
	Surface area	129.673	110.578
	Lipinski violations	1	1
	Bioavailability Score	0.55	0.55
	PAINS #alerts	0	0
	Brenk #alerts	0	0
	Synthetic Accessibility	2.72	2.38
	GI absorption	Low	Low
	MLOGP	7.38*	6.68*
Bioactivity scan	GPCR ligand	-0.04	-0.21
	Ion channel modulator	0.00	-0.01
	Kinase inhibitor	-0.14	-0.34
	Nuclear receptor ligand	-0.05	-0.25
	Protease inhibitor	0.11	-0.31
	Enzyme inhibitor	0.03	-0.04
Drug- likeness	MolLogP	10.90	9.38
	MolLogS	-6.26	-6.26
	MolPSA	0.00 A^2	0.00A^2
	MolVol	364.98 A^3	311.26A^3
	pK_a of most Basic/Acidic group	<0. / 25.39	<0. / 25.39
	BBB score	1.34	1.31
	Number of stereo centers	0	0
	Drug-likeness model score	-1.03	-1.03

In the case of the boiled egg method, it is assumed that points located in the yolk region pass the blood-brain barrier, while points in the white region are absorbed in the GI tract. PGP+ and PGP- points predict the possibility of discharge or no discharge by P-glycoprotein respectively, from the CNS. The results shown in **Figure 7** depict the position of the red point for heptadecane with BBB and GI absorption found to be negative along with PGP- portrayal of the molecule being elucidated by a high water partition coefficient value of 6.88. However, the molecule eicosane was not found to be placed in the boiled egg area with the corresponding water partition coefficient value of 8.05.

Bioavailability radar

Bioavailability radar is a descriptive and exemplified tool to explain the drug probability of selected ligands based on six physicochemical properties such as LIPO (lipophilicity), POLAR (polarity), INSOLU (insolubility), INSATU (saturation) and FLEX (flexibility). The study found that the alkane compounds eicosane and heptadecane were not orally bioavailable because the ligand array did not completely come under the pink-shaded area. Both the compounds were not orally bioavailable ligands as eicosane disobeyed the lipophilicity, insolubility, and flexibility parameters and heptadecane disobeyed lipophilicity and flexibility. The pictorial data is given below in **Figure 8**.

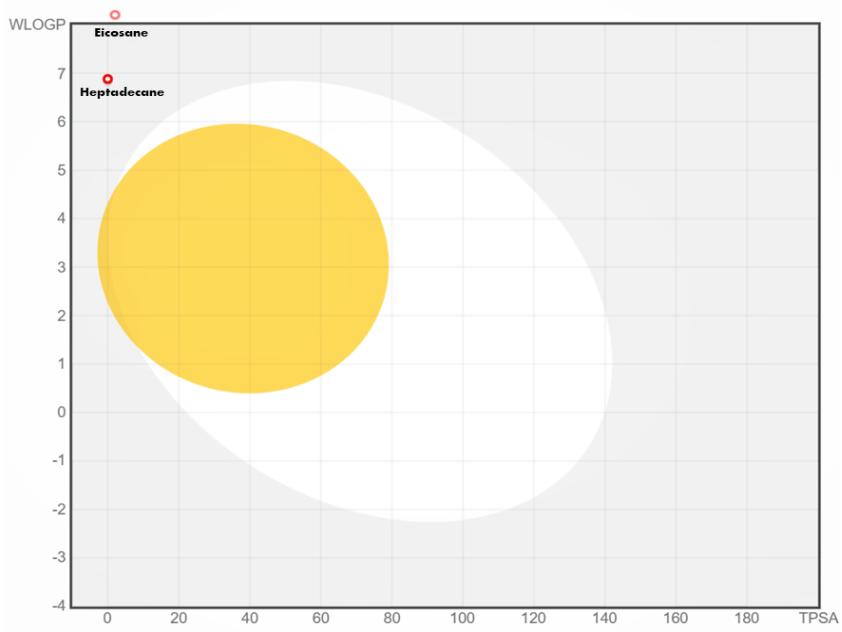

Figure 7. Boiled egg plot of the two selected long-chain alkanes (Eicosane and Heptadecane)

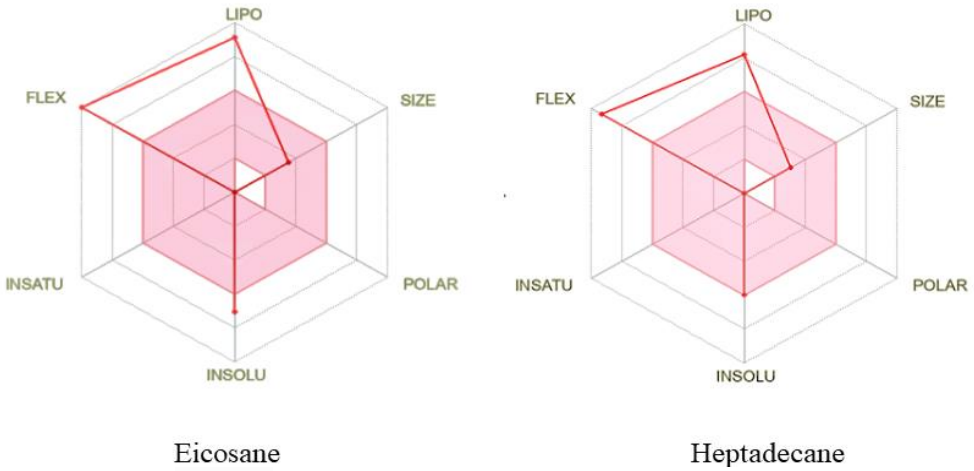

Figure 8. Bioavailability radar of Eicosane and Heptadecane

Molecular docking of eicosane and heptadecane with cyclooxygenase main proteases (COX-1 and COX-2)

Molecular docking is one of the primary tools to develop a novel drug. Alkanes such as eicosane and heptadecane are reported to have anti-inflammatory effects. So, encouraged by this anti-inflammatory activity, we selected these two compounds for molecular docking cyclooxygenase main proteases like COX-1 and COX-2. Docking is employed to find the binding affinity and the more negative values represent strong binding between drugs and proteins. In our study, we have found that compared to the standard drug (Ibuprofen), eicosane showed greater binding affinity but heptadecane showed less binding affinity against both the proteins. Ibuprofen showed a binding affinity of -6.1 Kcal/mol and -6.8 Kcal/mol against COX-1 (6Y3C) and COX-2 (5F19) respectively whereas, eicosane showed a binding affinity of -12Kcal/mol to COX-1 and -11 Kcal/mol to COX-2, and heptadecane has shown binding affinity of -5.5 Kcal/mol and -5.2 Kcal/mol against COX-1 and COX-2 (**Table 4**). A thorough study revealed that eicosane interacted with residues of the Cyclooxygenase-1 protein of Leu384(A), Phe518(A), Met522(A), Val349(A), Tyr355(A),

Val116(A), Leu359(A), Met113(A), Leu357(A), Arg120(A), Ala527(A), Gly526(A), Trp387(A) and heptadecane was found to be involved with Val116(A), Leu359(A), Val349(A), Ala527(A), Ser530(A), Gly526(A), Trp387(A), Leu352(A), Leu522(A), Ile523(A), Ser353(A), Phe518(A), Tyr355(A), Arg120(A), Leu357(A). In case of cyclooxygenase-2, molecular interaction of eicosane involved the amino acid residues Arg469(B), Glu465(B), Leu152(B), His39(B), Cys36(B), Asn34(B), Pro156(B), Pro153(B), Gln461(B), Lys468(B) and heptadecane interacted with Cys36(B), Tyr130(B), Pro153(B), Gly45(B), Leu152(B), Arg469(B), Arg44(B), Cys41(B), Glu465(B), Gln461(B), Cys47(B), His39(B), Gly135(B). Molecular docking interaction is given in **Figure 9** and **Figure 10**.

Molecular docking of eicosane and heptadecane with human Interleukin-6

The binding energy affinity of these two long-chain hydrocarbons against human Interleukin-6 (1ALU) have been concise in **Table 4**, where the molecular binding affinity was assessed to be more than -4.1 Kcal/mol compared to binding affinity of the standard drug ibuprofen which was found to be -5.2 Kcal/mol. Eicosane interacted with Lys27(A), Gln28(A), Tyr31(A), Val121(A), Met117(A), Ser1189A), whereas another query compound heptadecane was associated with Tyr31(A), Lys27(A), Arg30(A), Tla300(A), Gln175(A), Leu33(A), Asp34(A). Molecular interaction is shown in **Figure 11**.

Molecular docking of eicosane and heptadecane with Tumor necrosis factor-α

In case of Tnf- α (5MU8), the binding score of ibuprofen was found to be -6.4 Kcal/mol which is lower than the binding score of eicosane (-10.1 Kcal/mol) but higher than the heptadecane (-4.4 Kcal/mol) (**Table 4**) and the graphical interaction is provided in **Figure 12**, where eicosane was associated with the residues of Gly148(H), Val150(H), Pro20(H), Asn19(H), Pro139(H), Gly24(H), Leu142(H), Phe144(H), Ala18(H) and heptadecane was involved with Gly24(H), Glu135(D), Asn46(D), Leu26(D), Ile136(D), Gly24(D), Pro139(D), Arg138(H), Asp140(H), Asp45(D).

Table 4. Interaction profiling of concerned compounds with COX-1, COX-2, IL-6 and TNF-α proteins

	Eicosane		**Heptadecane**	
Receptor (**PDB ID**)	**Binding affinity (Kcal/mol)**	**Interacting residues**	**Binding affinity (Kcal/mol)**	**Interacting residues**
Cyclooxygenase-1 (**6Y3C**)	-12	Leu384(A), Phe518(A), Met522(A), Val349(A), Tyr355(A), Val116(A), Leu359(A), Met113(A), Leu357(A), Arg120(A), Ala527(A), Gly526(A), Trp387(A)	-5.5	Val116(A), Leu359(A), Val349(A), Ala527(A), Ser530(A), Gly526(A), Trp387(A), Leu352(A), Leu522(A), Ile523(A), Ser353(A), Phe518(A), Tyr355(A), Arg120(A), Leu357(A)
Cyclooxygenase-2 (**5F19**)	-11	Arg469(B), Glu465(B), Leu152(B), His39(B), Cys36(B), Asn34(B), Pro156(B), Pro153(B), Gln461(B), Lys468(B)	-5.2	Cys36(B), Tyr130(B), Pro153(B), Gly45(B), Leu152(B), Arg469(B), Arg44(B), Cys41(B), Glu465(B), Gln461(B), Cys47(B), His39(B), Gly135(B)
Interleukin-6 (**1ALU**)	-8.1	Lys27(A), Gln28(A), Tyr31(A), Val121(A), Met117(A), Ser1189A)	-4.2	Tyr31(A), Lys27(A), Arg30(A), Tla300(A), Gln175(A), Leu33(A), Asp34(A)
Tumor necrosis factor (**5MU8**)	-10.1	Gly148(H), Val150(H), Pro20(H), Asn19(H), Pro139(H), Gly24(H), Leu142(H), Phe144(H), Ala18(H)	-4.4	Gly24(H), Glu135(D), Asn46(D), Leu26(D), Ile136(D), Gly24(D), Pro139(D), Arg138(H), Asp140(H), Asp45(D)

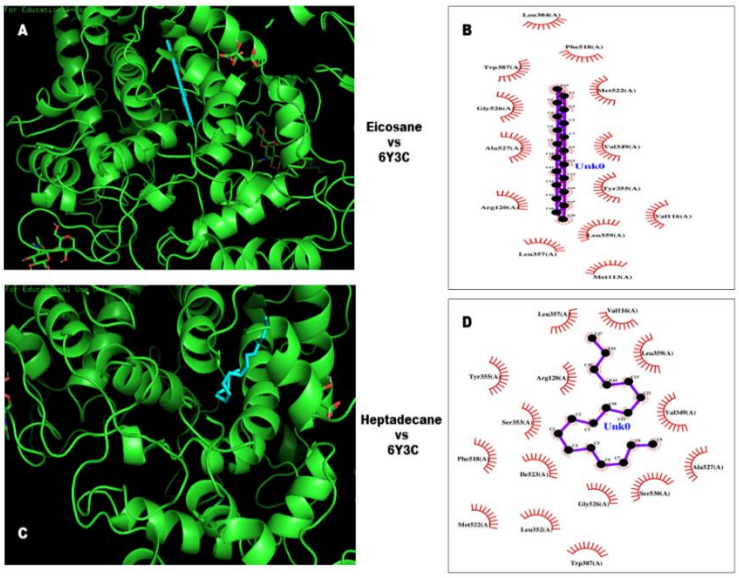

Figure 9. Molecular docking and interaction of Eicosane and Heptadecane with human Cyclooxygenase-1 protein, where A and C represent the docking against 6Y3C by Eicosane and Heptadecane respectively and B and D depict the interaction of 6Y3C by Eicosane and Heptadecane respectively

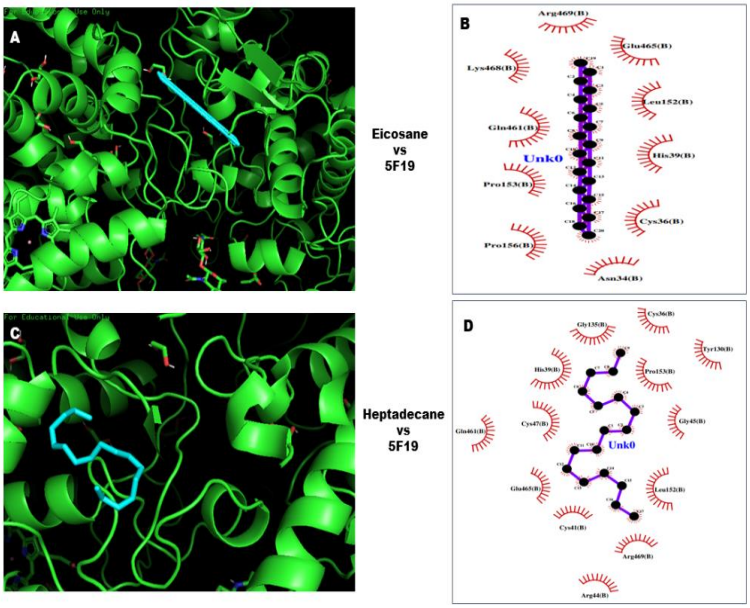

Figure 10. Molecular docking and interaction of Eicosane and Heptadecane with human Cyclooxygenase-2 protein, where **A** and **C** represent the docking against 5F19 by Eicosane and Heptadecane respectively and **B** and **D** depict the interaction of 5F19 by Eicosane and Heptadecane respectively

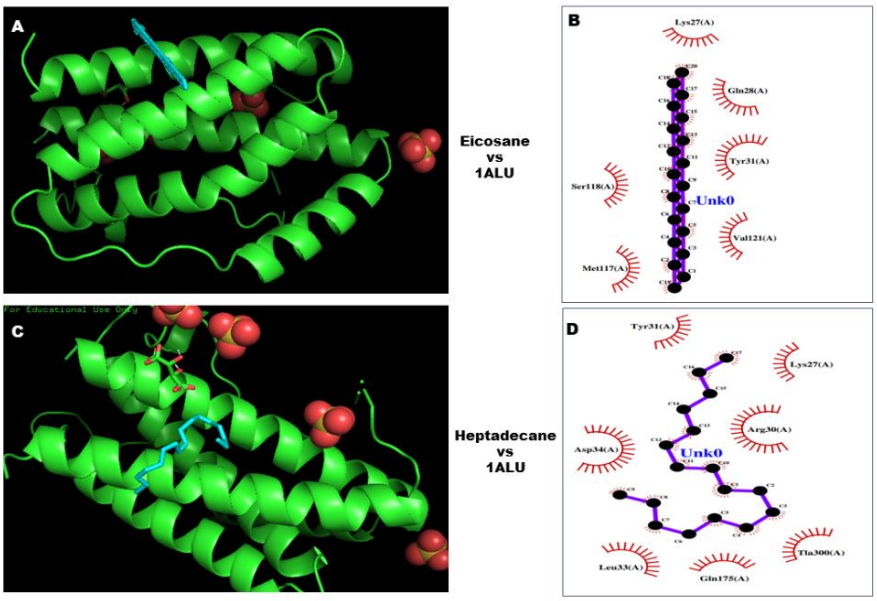

Figure 11. Molecular docking and interaction of Eicosane and Heptadecane with Interleukin-6 protein, where **A** and **C** represent the docking against 1ALU by Eicosane and Heptadecane respectively and **B** and **D** depict the interaction of 1ALU by Eicosane and Heptadecane respectively

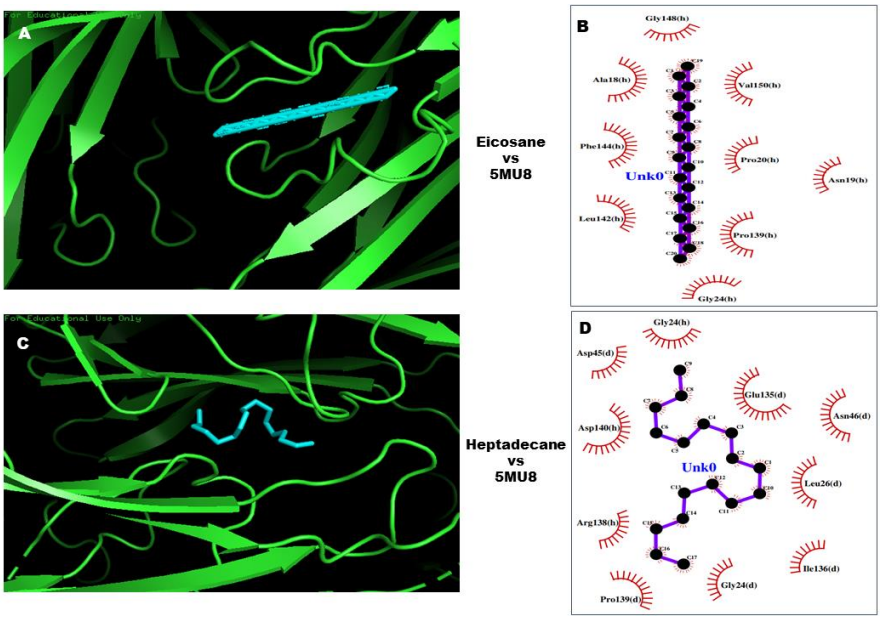

Figure 12. Molecular docking and interaction of Eicosane and Heptadecane with Tumor necrosis alpha protein, where **A** and **C** represent the docking against 5MU8 by Eicosane and Heptadecane respectively and **B** and **D** depict the interaction of 5MU8 by Eicosane and Heptadecane respectively

Biosynthesis pathway design through metabolomics and *in silico* study are valuable and potent techniques for the chemical and pharmacological standardization of plant extracts. It has the potential to revolutionize research on natural products and promote the scientific development of herbal-based therapy. This plant's compounds with their probable bioactivity through *in silico* study, have given us an idea about their mechanism of action while the

metabolomics of the selected compounds have disclosed the probable biosynthesis pathway of the compounds. So, this study might help the scientific community in the possible exploration of natural anti-inflammatory drugs. Furthermore, it is important to carry out *in vitro*, preclinical and clinical investigations, in order to advance the creation of novel pharmaceutical products.

Conclusion

Inflammation is an indication of many chronic diseases like arthritis or Alzheimer's disease, which affect human beings. There is always a huge demand for drugs to treat these disorders. As herbal remedies are gaining popularity due to their few side effects, our GC-MS analysis and *in silico* studies show that *Senna siamea* should not only be cultivated as a protective plant in this area but can also be used as a probable anti-inflammatory agent. It was observed that out of the 21 compounds detected in the *Senna siamea* leaf extract, twelve were long chain hydrocarbons and four were terpenoids. These compounds accounted for 57% and 19% of the total area, respectively. The most abundant alkane compounds were eicosane, heneicosane, and heptadecane, with peak areas of 4.38%, 3.45%, and 3.13% respectively. These findings provide important insights into the biosynthesis pathway of common plants that have not been previously explored. The findings of this metabolite-based pathway and *in silico* study need to be confirmed by other experiments like *in vitro* and *in vivo* studies, along with gene sequencing studies, to identify the main enzymatic genes involved in the synthesis of those anti-inflammatory alkanes distinguished in the extracts of *Senna siamea*. The molecular docking results of eicosane and heptadecane too exhibited significant protein-ligand interaction energy. This plant's extract contains substantial amounts of long-chain alkanes and terpenoids that can be utilized for many beneficial purposes. The separation and purification of both the compounds, followed by various analyses, could provide the basis for identifying new anti-inflammatory drugs.

Acknowledgement

The authors would like to acknowledge Sahadeb Sarkar for his help during the sample collection.

Funding

The research was partially funded by a University Research Grant (1506/R-2020)

Conflict of interest

The authors state that they do not have any conflict of interest.

References

Ahmed, A.H., Abdul, L.K., Najeeb, U.R., René, C. (2021). Biosynthetic diversity in triterpene cyclization within the *Boswellia* genus. *Phytochemistry*, 184. http://doi.org/10.1016/j.phytochem.2021.112660

Brown, A.P., Slabas, A.R., Rafferty, J.B. (2009). Fatty Acid Biosynthesis in Plants — Metabolic Pathways, Structure and Organization. In: Wada, H., Murata, N. (eds) *Lipids in Photosynthesis. Advances in Photosynthesis and Respiration*, vol 30, Springer, Dordrecht. https://doi.org/10.1007/978-90-481-2863-1_2

Chakraborty, S., Majumder, S., Ghosh, A., & Bhattacharya, M. (2022). Comprehensive profiling of aroma imparting biomolecules in foliar extract of *Hibiscus fragrans* Roxburgh: a metabologenesis perspective. *Journal of Biomolecular Structure and Dynamics*, 40(20), 10345-10358. http://doi.org/10.1080/07391102.2021.1943525

Garg, S., Anand, A., Lamba, Y., & Roy, A. (2020). Molecular docking analysis of selected phytochemicals against SARS-CoV-2 M pro receptor. *Vegetos*, 33, 766-781. https://doi.org/10.1007/s42535-020-00162-1

Ghosh, A., Chakraborty, S., Majumder, S., & Bhattacharya, M. (2022). Comprehensive *In silico* Investigation Validates Two Flavonoid Compounds of *Derris robusta* (Roxb. ex DC.) Benth. to Supplant Remdesivir as Natural Therapeutic Remedy Against a Range of Coronaviruses. *Letters in Applied NanoBioscience*, 12(4). https://doi.org/10.33263/LIANBS124.108

Ghosh, A., Majumder, S., Saha, S., Sarkar, S., & Bhattacharya, M. (2021). Gas Chromatography-Mass Spectrometry profiling, and evaluation of antioxidant and antibacterial activity of *Albizia* spp. *Nusantara Bioscience*, 13(2). https://doi.org/10.13057/nusbiosci/n130207

Gunalan, G., Vijayalakshmi, K., Saraswathy, A., Hopper, W., & Tamilvannan, T. (2014). Anti-inflammatory activities of phytochemicals from *Bauhinia variegata* Linn. leaf: An *in-silico* approach. *Journal of chemical and pharmaceutical research*, *6*(9), 334-48.

Hanuš, L.O., Arieh, M., Tomáš, Ř., Saleh, A.L., and Valery, M.D. (2007). Phytochemical analysis and comparison for differentiation of *Boswellia carterii* and *B. Serrata*. *Natural Product Communications*, 2(2). https://doi.org/10.1177/1934578X0700200206

Hassan, S.S.U., Zhang, W.D., Jin, H.Z., Basha, S.H., & Priya, S.S. (2022). *In-silico* anti-inflammatory potential of guaiane dimers from *Xylopia vielana* targeting COX-2. *Journal of Biomolecular Structure and Dynamics*, *40*(1), 484-498. https://doi.org/10.1080/07391102.2020.1815579

Hildebrandt, T.M., Nunes-Nesi, A., Araujo, W.L., & Braun, H.P. (2015). Amino acid catabolism in plants. *Molecular Plant*, 8(11), 1563–1579. https://doi.org/10.1016/j.molp.2015.09.005

Iqbal, T., Chakraborty, S., Murugan, S., & Das, D. (2022). Metalloenzymes for Fatty Acid-Derived Hydrocarbon Biosynthesis: Nature's Cryptic Catalysts. *Chemistry–An Asian Journal*, 17(10), e202200105. https://doi.org/10.1002/asia.202200105

Joshi, T., Sharma, P., Joshi, T., & Chandra, S. (2020). *In silico* screening of anti-inflammatory compounds from Lichen by targeting cyclooxygenase-2. *Journal of Biomolecular Structure and Dynamics*, *38*(12), 3544-3562. https://doi.org/10.1080/07391102.2019.1664328

Kamagaté, M., Koffi, C., Kouamé, N. M., Akoubet, A., Alain, N., Yao, R., & Die, H. (2014). Ethnobotany, phytochemistry, pharmacology and toxicology profiles of *Cassia siamea* Lam. *The Journal of Phytopharmacology*, 3(1), 57-76.

Kumar, D., Jain, A., & Verma, A. (2017). Phytochemical and pharmacological investigation of *Cassia siamea* Lamk: An insight. *The Natural Products Journal*, 7(4), 255-266. http://dx.doi.org/10.2174/2210315507666170509125800

Lucas, K.A., Filley, J.R., Erb, J.M., Graybill, E.R., & Hawes, J.W. (2007). Peroxisomal metabolism of propionic acid and isobutyric acid in plants. *The Journal of Biological Chemistry*, 282(34), 24980–24989. https://doi.org/10.1074/jbc.M701028200

Majumder, S., Ghosh, A., & Bhattacharya, M. (2020). Natural anti-inflammatory terpenoids in Camellia japonica leaf and probable biosynthesis pathways of the metabolome. *Bulletin of the National Research Centre*, 44(1), 1-14. https://doi.org/10.1186/s42269-020-00397-7

Majumder, S., Ghosh, A., Saha, S., Acharyya, S., Chakraborty, S., Sarkar, S., & Bhattacharya, M. (2022). Valorization of CTC tea waste through kombucha production and insight into GC-MS based metabolomics. *Canrea Journal: Food Technology, Nutritions, and Culinary Journal*, 5(1), 38-56. https://doi.org/10.20956/canrea.v5i1.594

Mehta, J.P., Parmar, P.H., Vadia, S.H., Patel, M.K., & Tripathi, C.B. (2017). *In-vitro* antioxidant and *in-vivo* anti-inflammatory activities of aerial parts of *Cassia* species. *Arabian Journal of Chemistry*, *10*, S1654-S1662. https://doi.org/10.1016/J.ARABJC.2013.06.010

Priya, R., Sumitha, R., Doss, C., Rajasekaran, C., Babu, S., Seenivasan, R., Siva, R. (2015) Molecular docking and molecular dynamics to identify a novel human immunodeficiency virus inhibitor from alkaloids of *Toddalia asiatica*. *Pharmacognosy Magazine*, 11, S414–422. https://doi.org/10.4103/0973-1296.168947

Schneider-Belhaddad, F., & Kolattukudy, P. (2000). Solubilization, partial purification, and characterization of a fatty aldehyde decarbonylase from a higher plant, *Pisum sativum*. *Archives of biochemistry and biophysics*, 377(2), 341-349. https://doi.org/10.1006/abbi.2000.1798

Shaik, N.A., Al-Kreathy, H.M., Ajabnoor, G.M., Verma, P.K., Banaganapalli, B. (2019) Molecular designing, virtual screening and docking study of novel curcumin analogue as mutation (S769L and K846R) selective inhibitor for EGFR. *Saudi journal of biological sciences*, 26, 439-448. https://doi.org/10.1016/j.sjbs.2018.05.026

Sukma, M., Chaichantipyuth, C., Murakami, Y., Tohda, M., Matsumoto, K., Watanabe, H. (2002). CNS inhibitory effects of barakol, a constituent of *Cassia siamia* Lamk. *Journal of ethnopharmacology*, 83(1-2), 87-94. https://doi.org/10.1016/S0378-8741%2802%2900206-4

Veerachari, U., & Bopaiah, A.K. (2011). Preliminary phytochemical evaluation of the leaf extract of five *Cassia* species. *Journal of Chemical and Pharmaceutical research*, 3(5), 574-583.

Yan, H., Wang, Z., Wang, F., Tan, T., & Liu, L. (2016). Biosynthesis of chain-specific alkanes by metabolic engineering in *Escherichia coli*. *Engineering in Life Sciences*, 16(1), 53-59. https://doi.org/10.1002/elsc.201500057